Plant Physiology Preview. Published on November 27, 2013, as DOI:10.1104/pp.113.225144

Running head:
miR396 and pistil development

Author to whom all correspondence should be sent:
Diqiu Yu
Key Laboratory of Tropical Forest Ecology, Xishuangbanna Tropical Botanical Garden, Chinese Academy of Sciences, Kunming, Yunnan 650223, China.
Tel: 86-871-65178133
Fax: 86-871-65160916
E-mail: ydq@xtbg.ac.cn

Research Area:
Genes, Development and Evolution

Molecular mechanism of miR396 mediating pistil development in *Arabidopsis thaliana*

One-sentence summary:

miR396 mediates pistil development by suppression of its *GRF* target genes to impair the formation of GRF/GIF co-transcription complex.

Gang Liang[1], Hua He[1,2], Yang Li[1,2], Fang Wang[1], and Diqiu Yu[1]*

[1]Key Laboratory of Tropical Forest Ecology, Xishuangbanna Tropical Botanical Garden, Chinese Academy of Sciences, Kunming, Yunnan 650223, China.

[2]University of Chinese Academy of Sciences, Beijing 100049, China.

Footnotes:

This work was supported by the Natural Science Foundation of China [31100186], the West Light Foundation of CAS, and the CAS 135 program [XTBG-F04].

Correspondence author: Diqiu Yu, ydq@xtbg.ac.cn

ABSTRACT

The precise control of gene regulation, and hence, correct spatio-temporal tissue patterning, is crucial for plant development. Plant microRNAs can constrain the expression of their target genes at post-transcriptional levels. Recently, miR396 has been characterized to regulated leaf development by mediating cleavage of its *GRF* targets. miR396 is also preferentially expressed in flowers. However, its function in flower development is unclear. In addition to narrow leaves, pistils with a single carpel were also observed in miR396 over-expression plants. The dramatically reduced expression levels of miR396 targets (*GRF1, 2, 3, 4, 7, 8, and 9*) caused pistil abnormalities, because the miR396-resistant version of *GRF* was able to rescue miR396-over-expressing plants. Both *GRF*s and *GIF*s are highly expressed in developing pistils, and their expression patterns are negatively correlated with that of miR396. GRF interacted with GIF to form the GRF/GIF complex in plant cell nucleus. miR396 suppressed the expression of *GRF*s, resulting in reduction of GRF/GIF complex. *gif* single mutant displayed normal pistils whereas *gif* triple mutant, *gif1/gif2/gif3*, produced abnormal pistils, which was a phenocopy of *35S:MIR396a/grf5* plants. GRF and GIF function as co-transcription factors and both are required for pistil development. Our analyses reveal an important role for miR396 in controlling carpel number and pistil development via regulation of the GRF/GIF complex.

INTRODUCTION

The precise spatial and temporal expression of regulatory genes that control tissue patterning and cell fate is important for plant development. Mis-expression of certain key regulatory genes causes developmental abnormalities in plants. There is increasing evidence that small RNA molecules are important participants in the control of gene expression, providing sequence specificity for targeted regulation of key developmental factors at the post-transcriptional level. MicroRNAs (miRNAs) are 21–24 nt non-coding RNAs that negatively regulate gene expression by pairing with their target mRNAs. They are produced from primary miRNAs (pri-miRNAs) that are transcribed from MIRNA genes. After the miRNAs duplexes are released from the nucleus, mature miRNAs are recruited into an RNA-induced silencing complex (RISC) associated with ARGONAUTE (AGO) proteins, where they suppress target mRNAs by complementary matching for cleavage and (or) translational repression (Reinhart et al., 2002; Carrington and Ambros, 2003; Bartel, 2004; Brodersen et al., 2008; Lanet et al., 2009).

Several plant miRNAs have been shown to function in plant development. The lack of miRNA processing protein(s) can cause severe developmental phenotypes. For example, the weaker *dcl1* alleles produce various aberrant morphological phenotypes, including extra whorls of stamens, an indefinite number of carpels, female sterility, altered ovule development, and reduced plant height, indicating that miRNA metabolism is essential for normal plant development (Schauer et al., 2002). *ago1* null mutants exhibit morphological defects similar to those of *dcl1*, *hen1*, and *hyl1* mutants (Vaucheret et al., 2004). The specific functions of miRNAs in floral development have been characterized. For example, *Arabidopsis* miR160a mutant produced floral organs in carpels (Liu et al., 2010). Over-expression of miR164 led to flowers with fused sepals, which resembled the flowers of its target mutants, *cuc1cuc2* (Mallory et al., 2004). Enhanced expression of the miR164-resistant version of *mCUC1* resulted in flowers with more petals than those of wild-type (Baker et al., 2005). Plants ectopically expressing miR166 showed extreme fasciation of the inflorescence meristem and a reduced or filamentous gynoecium (Kim et al., 2005; Williams et al., 2005). Constitutive expression of miR159 or miR167,

which led to reduced expressions of their target genes (*MYB33* and *MYB65*; *ARF6* and *ARF8*), caused male sterility in *Arabidopsis* (Achard et al., 2004; Millar and Gubler, 2005; Ru et al., 2006; Wu et al., 2006). Elevated miR172 accumulation resulted in floral organ identity defects similar to those in its target gene mutant (*apetala2*) (Aukerman and Sakai, 2003; Chen, 2004).

*GROWTH-REGULATING FACTOR*s (*GRF*s) are a class of plant-specific transcription regulators. In *Arabidopsis* there are nine *GRF* genes that can be divided into five sub-families; Group I (*GRF1* and *GRF2*), Group II (*GRF3* and *GRF4*), Group III *(GRF5* and *GRF6*), Group IV (*GRF7* and *GRF8*), and Group V (*GRF9*) (Kim et al., 2003). Among them, *GRF1, 2, 3, 4, 7, 8,* and *9* are the direct targets of miR396 (Jones-Rhoades and Bartel, 2004). It has been revealed that miR396 is involved in leaf development by controlling the levels of its *GRF* targets (Liu et al., 2009; Yang et al., 2009; Rodriguez et al., 2010; Wang et al., 2011; Debernardi et al., 2012). A GRF protein consists of two regions, the QLQ and WRC domains. The QLQ domain is responsible for protein interaction, while the WRC domain comprises a functional nuclear localization signal and a zinc-finger motif that functions in DNA binding (Kim et al., 2003). *GRF* genes are involved in regulating leaf growth and morphology (Kim et al., 2003; Horiguchi et al., 2005). The GRF-INTERACTING FACTOR 1 (GIF1) protein was identified to interact with GRF1 as a transcription co-activator to regulate leaf development (Kim et al., 2004). Horiguchi et al. (2005) revealed that both GRF5 and GRF9 interact with GIF1 to regulate leaf development. GIF1 contains two domains; the SNH and QG domains. The SNH domain is responsible for the interaction with the QLQ domain of GRF. The *GIF* gene family has three members, *GIF1*, *GIF2*, and *GIF3*, which have overlapping functions in determining organ (leaf and petal) size (Kim et al., 2004; Lee et al., 2009).

Another group (Hewezi et al., 2012) revealed the functions of miR396 in reprogramming root cells during infection by a parasitic cyst nematode. Here, we demonstrate that the products of all 7 *GRF* targets can interact with GIFs that may function as co-transcription factors. Over-expression of miR396 caused reduced expressions of *GRF* genes, which disrupted the formation of the GRF/GIF complex, leading to pistil anomalies. These results indicate that miR396-directed regulation is critical for pistil development.

RESULTS

Over-expression of miR396 resulted in aberrant pistils

Two *MIR396*-gene-encoding loci (*MIR396a* and *MIR396b*) have been identified in *Arabidopsis*. They are processed into two types of mature miR396s with only one nucleotide difference (Jones-Rhoades and Bartel, 2004). In our previous research, we found that miR396 was ubiquitously expressed in seedlings, roots, leaves, siliques, and inflorescences, and that constitutive expression of miR396 caused narrow leaves by targeting *GRF* genes in *Arabidopsis* (Liu et al., 2009). Further investigation found that miR396-overexpressing plants produced flowers with various deformations. Wild-type flowers often contain four sepals, four petals, six stamens, and two fused carpels (Fig. 1A). In miR396-overexpressing plants, approximately 70% of flowers contained aberrant pistils, such as extremely bent pistils, unfused carpels, and single carpels (Fig. 1B–D). The aberrant pistils formed into short siliques (Fig. 1E). The single-carpel siliques contained only one column of seeds (Fig. 1F), which accounted for approximately 65% of all siliques (Fig. 1G). The abnormal siliques resulted in lower fertility compared with that of wild-type (Fig.1H).

Given the fact that increased levels of miR396 led to aberrant pistils, we asked what would happen when miR396 expression was repressed. To suppress the functions of both miR396a and miR396b, we used the Short Tandem Target Mimic (STTM) strategy (Yan et al., 2012) to construct *STTM396*-transgenic plants. Northern blotting analysis indicated that miR396 was moderately decreased in the flowers of *STTM396* plants (Fig. S1A). However, the pistils and siliques of *STTM396* plants were normal (Fig. S1B).

miR396 suppressed expression of *GRF* genes in floral organs

In *Arabidopsis*, there are nine *GRF* genes, seven of which are predicted to be targeted by miR396. The cleavage of six *GRF*s (*GRF1*, *2*, *3*, *7*, *8*, and *9*) has been validated experimentally (Jones-Rhoades and Bartel, 2004). We confirmed the cleavage of *GRF4* in the predicted miR396 recognition site by 5’RACE experiments (Fig. S2A).

We compared the transcript levels of *GRF* genes in flowers among wild-type,

35S:MIR396a, and *STTM396* plants; the level of miR396 was negatively correlated with those of its *GRF* targets (Fig. 2A). Unexpectedly, two non-targeted *GRF*s were affected differently by miR396. Like the other targeted *GRF*s, the level of *GRF6* transcripts was negatively correlated with that of miR396. In contrast, the transcript level of *GRF5* was not influenced by miR396. The levels of *GRF*s transcripts and miR396 were further examined in different floral organs of wild-type. The lowest level of miR396 and the highest levels of *GRF*s transcripts were in the pistil (Fig. 2B). Considering the high frequency of altered pistils in miR396-overexpressing plants, we investigated the levels of *GRF*s transcripts and miR396 in the pistils of flowers at three different developmental stages (Fig. 2C). There were relatively high transcript levels of *GRF*s at stages 10 and 13, but low levels at stage 15. In contrast, the transcript levels of both *MIR396*a and *MIR396b* were relatively low at stages 10 and 13, but high at stage 15. Taken together, these results indicated that miR396 may constrain the expression of *GRF* genes.

To confirm the direct regulation of *GRF* genes by miR396 *in planta,* we performed transient co-expression assays in *Nicotiana bethamiana*. We generated two types of constructs for both *GRF7* and *GRF9*, the miR396-sensitive constructs *35S:GRF7* and *35S:GRF9* and the miR396-resistant constructs *35S:mGRF7* and *35S:mGRF9*. The miR396-resistant version of *mGRF* contained three silent mutations within the miR396-complementary domain of the *GRF* genomic clone, thereby increasing the number of mismatches between miR396 and *mGRF* without altering the amino acid sequence of the encoded GRF protein (Fig. S2B). After 3 days of co-expression in *N. benthamiana*, RNA was extracted and the transcript abundances of *GRF7* and *GRF9* were analyzed by real-time quantitative RT-PCR. The mRNA levels of miR396-resistant *mGRF7* or *mGRF9* were not affected by co-expression with MIR396a. However, mRNA levels of the miR396-sensitive *GRF7* and *GRF9* were significantly decreased when co-expressed with MIR396a (Fig. 2D). These findings suggested that miR396 directly mediates the cleavage of *GRF* genes *in planta*.

miR396-resistant *mGRF7* or *mGRF9* rescued miR396 transgenic plants

Analyses of the expression patterns of *GRF* genes showed that all nine *GRF*

genes are expressed in roots, upper stems, and shoot tips containing the shoot apical meristem and flower buds, as well as in mature flowers (Kim et al., 2003). Because *GRF* genes are suppressed by miR396, we expected that *GRF* mutants could phenocopy miR396-overexpressing plants. We obtained six *GRF* single-mutants (Fig. S3A), *grf1*, *grf3*, *grf4*, *grf7*, *grf8*, and *grf9*, all of which produced normal siliques (Fig. S3B). The *grf1grf2grf3* triple mutants (Ws background) (Kim et al., 2003) have small leaves, but normal floral organs and fertility. The leaves of the *grf7* single mutant were reported to be smaller than those of wild-type (Kim et al., 2012), implying that Group IV *GRF* genes may play a dominant role. Therefore, we constructed a *grf7grf8* double mutant and a *grf7grf8grf9* triple mutant. These mutants produced normal siliques (Fig. S3B). In flowers of miR396-overexpressing plants, all *GRF* genes except for *GRF5* were down-regulated (Fig. 2A). We could not investigate the individual functions of the *GRF* genes because of the 8-fold redundancy and their overlapping expression patterns. It was also very difficult to obtain an octuple mutant for the eight down-regulated *GRF* genes because of their close linkages on chromosomes.

To investigate whether reduced expressions of *GRF* genes caused the aberrant pistils of miR396-overexpressing plants, we conducted functional complementation tests. Each of four *GRF* constructs (*35S:GRF7*, *35S:mGRF7*, *35S:GRF9*, and *35S:mGRF9)* was transformed into *Arabidopsis* wild-type plants. All transgenic plants produced normal siliques (Fig. S3C). When *35S:GRF7-* or *35S:GRF9*-plants were crossed with *35S:MIR396*a-plants, their progenies (*35S:GRF7*/*35S:miR396a* or *35S:GRF9*/*35S:miR396a*) still formed abnormal pistils and single-carpel siliques, although there were smaller proportions of abnormal siliques. In contrast, when *35S:mGRF7-* or *35S:mGRF9*-plants were crossed with *35S:MIR396a*-plants, their progenies (*35S:mGRF7*/*35S:miR396a* or *35S:mGRF9*/*35S:miR396a*) developed normal siliques (Fig. 3A). We further quantified the transcript levels of *GRF7* and *GRF9* in F1 progenies (Fig. 3B). As expected, the level of *GRF7* transcripts was dramatically decreased in *35S:GRF7*/*35S:miR396a*-plants, compared with that in *35S:GRF7*/WT plants. In contrast, the levels of *GRF7* transcripts in *35S:mGRF7*/*35S:miR396a*-plants were similar to that in *35S:mGRF7*/WT plants. A similar case was also observed for *GRF9*. Therefore,

miR396-resistant *mGRF7* and *mGRF9,* but not miR396-sensitive *GRF7* and *GRF9*, were sufficient to recover *35S:MIR396a*. Our results suggested that the reduced expressions of *GRF* genes were responsible for the pistil abnormalities of miR396-overexpressing plants.

GRF interacted with GIF as co-transcription factors

Previous studies demonstrated that GRF1 and GIF1 function as co-transcription factors in regulating leaf growth and morphology in *Arabidopsis* (Kim and Kende, 2004). In *Arabidopsis*, there are two homologs (GIF2 and GIF3) of GIF1. To determine whether each GRF protein can interact with each GIF protein, we used yeast-two hybridization (Y2H) assays to investigate their interactions. As shown in Fig. 4A, GIF1 strongly interacted with seven GRFs, but only weakly interacted with GRF4 and GRF7. In contrast, both GIF2 and GIF3 strongly interacted with all GRFs except for GRF9.

Next, we used bimolecular fluorescence complementation (BiFC) assays to verify these protein interactions *in planta*. The N-terminal fragment of yellow fluorescent protein (nYFP) was individually ligated with GRF4, GRF7, and GRF9 to produce GRF4-nYFP, GRF7-nYFP, and GRF9-nYFP, respectively. The GIF1, GIF2, and GIF3 proteins were individually fused with the C-terminal fragment of YFP (cYFP). When GIF1-cYFP was transiently co-expressed with GRF9-nYFP, strong YFP fluorescence was visible in the nucleus of epidermal cells in *N. benthamiana* leaves (Fig. 4B), whereas no YFP fluorescence was detected in negative controls (GIF1-cYFP co-expressed with nYFP or cYFP co-expressed with GRF9-nYFP) (Fig. S4). Similar results were observed for co-expression of GIF2-cYFP with GRF7-nYFP and GIF3-cYFP with GRF4-nYFP (Fig. 4B).

To further confirm whether GRF and GIF form protein complex in plant cells, we performed Co-Immunoprecipitation assays (Fig. 4C). GRF and GIF were transiently co-expressed in tobacco leaves. The total proteins were incubated with Flag antibody and A/G-agarose beads and then separated on SDS-PAGE for immunoblotting with Myc antibody. In agreement with the results in BiFC, GRF and GIF exist in the same protein complex. Taken together, our results suggested that GRFs and GIFs function as co-transcription factors.

Spatio-temporal expression of *GRF*s and *GIF*s in flowers

Our results demonstrated that GRF proteins can physically interact with GIF proteins. To serve as co-transcription factors in flowers, GRFs and GIFs must have the same spatio-temporal expression patterns. To determine their expression patterns, *Arabidopsis* was transformed with *promoter-β-glucuronidase* (*GUS*) fusion constructs for each of these 12 genes (Fig. 5A). In flowers, the *GRF3* promoter drove GUS expression in the receptacle and the *GRF8* promoter drove GUS expression in the anther. The remaining seven *GRF* gene promoters and three *GIF* gene promoters were mainly activated in the pistil, although they showed somewhat different spatial expression patterns.

We further analyzed the transcript levels of *GIF* genes in sepals, petals, stamens, and pistils. Like *GRF* genes (Fig. 2B, C), the highest levels of *GIFs* transcripts were in the pistil (Fig. 5B) and their expressions in the pistil decreased at later stages of flower development (Fig. 5C).

Suppression of *GRF*s by miR396 caused the reduction of GRF/GIF complex

Because *GRF*s are post-transcriptionally regulated by miR396, we expected that increased accumulation of miR396 would reduce the abundance of GRF/GIF complexes. To confirm our hypothesis, transient expression assays were conducted in *N. benthamiana* leaves (Fig. 6). When GIF2-cYFP and GRF7-nYFP were co-expressed with miR396a, only a few epidermal cells displayed visible YFP fluorescence. As a negative control, when they were co-expressed with miR395a, which cannot recognize the *GRF7* gene, many cells showed YFP fluorescence. When GIF2-cYFP and mGRF7-nYFP were co-expressed with miR396a, most cells showed strong YFP fluorescence. These results indicated that the suppressed GRF expression reduces the formation of GRF/GIF complex.

Phenotypes of *GIF* triple mutant, *gif1/2/3*, were similar to those of *35S:MIR396a/grf5* plants

Since GRF and GIF function as co-transcription factors, we expected that the *GIF* mutants would phenocopy miR396-overexpressing plants. Previous

studies (Kim et al., 2004) revealed that the *gif1* mutant produces narrow leaves similar to those of 35S:*MIR396a.* We examined the siliques of *gif1* mutants, and found that all of them contained two carpels, but they were significantly shorter than wild-type siliques. We speculated that *GIF1* would be functionally redundant with the other two *GIF* genes. To confirm our hypothesis, we constructed *gif1/2*, *gif1/3*, *gif2/3*, and *gif1/2/3* mutants by crossing *gif* single mutants (Fig. S5A). Compared with the siliques of the gif1 mutant, those of the *gif1/2* and *gif1/3* mutants were shorter but those of the *gif2/3* mutant were of a similar length. In contrast, the siliques of triple mutants were shorter than those of double mutants (Fig. S5B). The *gif1/2/3* triple mutant formed bent siliques, single-carpel siliques, and unfused-carpel siliques (Fig. 7A–D). However, there were markedly fewer single-carpel siliques in *gif1/2/3* mutants than in *35S:MIR396a* plants (Fig. 7E). In addition, *gif1/2/3* mutants showed very low fertility with no more than 20 seeds per plant, because most siliques did not contain seeds. This differed from *35S:MIR396a* plants, in which only about 10% of siliques did not contain seeds.

Although eight *GRF*s showed reduced transcript levels in *35S:MIR396a* plants, *GRF5* transcripts were not affected by miR396, which may have contributed to the higher fertility of *35S:MIR396a* plants compared with *gif1/2/3* mutants. To explore this idea, the *grf5* mutant was crossed with *35S:MIR396a* plants and *35S:MIR396a/grf5* plants were obtained by screening F2 plants. As expected, *35S:MIR396a/grf5* plants displayed lower fertility and had fewer single-carpel siliques than did *35S:MIR396a* plants, indicating that *35S:MIR396a/grf5* plants phenocopied *gif1/2/3* mutant plants (Fig. 7D, E).

DISCUSSION

miRNAs play a key role in regulating plant development, which can be inferred from the developmental defects in *dcl1*, *hyl1*, *se*, and *ago1* mutants, and from analyses of plants over-expressing various miRNAs (e.g., miR160, miR164, miR166, and miR319, etc.). Here, we demonstrated that over-expression of miR396 results in morphological defects in floral organs. Our results reveal the function of miR396 in reducing the formation of the GRF/GIF complex, which regulates pistil development.

Functional redundancies of *GRF* family members

Previously, we showed that over-expression of miR396 results in narrow rosette leaves and reduced expressions of its *GRF* target genes (Liu et al., 2009). Here, our results indicate that elevated miR396 also causes floral abnormalities by suppressing the expressions of its *GRF* target genes. The *Arabidopsis* genome contains nine *GRF* genes, all of which are expressed in leaves and flowers. However, only *grf5* and *grf7* single mutants produced leaves slightly smaller than those of wild-type plants (Horguchi et al., 2005; Kim et al., 2012), whereas the other *grf* single mutants displayed no developmental abnormalities. The *grf1/2/3* triple mutants produced small leaves and cotyledons, indicating that *GRF1*, *GRF2*, and *GRF3* participate redundantly in controlling leaf cell number (Kim et al., 2003). Previous investigations confirmed that over-expression of *GRF1*, *GRF2*, or *GRF5* can increase the leaf surface area (Kim et al., 2003; Horguchi et al., 2005). We found that plants overexpressing *GRF7* or *GRF9* showed slightly enlarged leaves (Fig. S6), but *grf7/8/9* mutants produced leaves similar to those of *grf7* single mutants, suggesting their overlapping functions in regulating leaf development. Our results revealed that the down-regulation of *GRF* genes is responsible for the aberrant siliques of miR396-overexpressing plants, because the miR396-resistant version of *GRF* could recover their silique phenotypes. Both *grf1/2/3* and *grf7/8/9* mutants produced normal siliques, indicating redundant functions of these *GRF* genes in regulating floral development. Although *GRF5* is not the target of miR396, a *grf5* mutation aggravated the abnormalities in leaves and siliques of *35S:MIR396a* plants (Fig. S7; Fig. 7D), indicating its redundant functions with other *GRF* genes. Interestingly, the introduction of *grf5* into *35S:MIR396a* plants reduced the number of single carpel siliques. Meanwhile, we also observed that it also led to nearly sterility. It seems that the single carpel ensures the production of necessary seeds. Further investigation is required to reveal the underlined mechanism. In addition, all of the *GRF* genes showed overlapping expression patterns in the flower, with their highest expression levels in the pistil. Taken together, these results showed that *GRF* genes function redundantly in regulating plant development.

GRF and GIF co-regulate pistil development

GRF proteins contain two conserved domains, QLQ and WRC, in their N-terminal region. The QLQ domain is very similar to the N-terminal part of the SWI2/SNF2 protein that interacts with another component of the SWI2/SNF2 chromatin-remodeling complex in yeast (Treich et al., 1995). The WRC domain consists of a functional nuclear localization signal and a DNA-binding motif. The C-terminal regions of GRFs have common features of transcription factors and are required for their transcription activation activities because N-terminal-truncated GRFs lose their transactivation functions (Fig. 4A). GIF proteins contain a SNH domain and a QG domain, which are similar to domains in the SYT protein, a transcriptional coactivator in human (Brett et al., 1997). The SYT protein can interact with SWI2/SNF2-chromatin remodeling proteins, which may regulate transcription via chromatin modification (Thaete et al., 1999; Kato et al., 2002; Aizawa et al., 2004). Similarly, our results indicated that GIF proteins can interact with GRF proteins in both yeast and plant cells. Thus, similar to the interaction between SYT and SWI2/SNF2 proteins, GIF interacts with GRF to influence the transcriptions of downstream target genes.

miR396-over-expressing plants, in which all of the *GRF* genes except for *GRF5* were dramatically down-regulated, produced abnormal pistils. The spatio-temporal expression patterns of *GRF* genes in the flower were very similar to those of *GIF* genes, and both were expressed at relatively high levels in the pistil. The combination of their expression patterns and their interactions in the plant cell nucleus implied that *GRF* and *GIF* may co-regulate pistil development. Our results revealed that each GIF protein can interact with almost all of the GRF proteins, implying that one GIF modulates the functions of multiple GRFs. That explains why *gif1* single mutants, but not *grf* single mutants, displayed short siliques. We also observed that siliques of *35S:MIR396a/grf5* were shorter than those of *35S:MIR396a* (Fig. 7E). The siliques of *gif* double mutants (*gif1/2* and *gif1/3*) were shorter than those of *gif1* mutants, and the siliques of *gif1/2/3* triple mutants were shorter than those of double mutants (Fig. S7B). Both *35S:MIR396a*/grf5 and *gif1/2/3* caused short and almost completely sterile siliques as well as single-carpel siliques,

suggesting that silique development is *GRF*-dose-dependent and *GIF*-dose-dependent.

Proper regulation of *GRF*s by miR396 is crucial for plant development

Several miRNAs have been shown to function in regulating floral development (Mallory et al., 2004; Williams et al., 2005; Achard et al., 2004; Wu et al., 2006; Chen, 2004), and all of these miRNAs are conserved across plant species. The mis-expression of these miRNAs followed by mis-expression of their targets can cause abnormal development of floral organs, suggesting that a balance between these miRNAs and their targets is required for floral development. Similarly, we demonstrated that over-expression of miR396 mediated the down-regulation of their *GRF* targets, resulting in abnormal floral organs. In wild-type flowers, all nine *GRF* genes were highly expressed at an early stage of pistil development, and their abundance decreased as the siliques mature. In contrast, both *MIR396a* and *MIR396b* genes were expressed at low levels in young siliques and their abundance increased as the siliques matured. The inverse correlation between miR396 and its targets implied that miR396 constrains the expression of its target genes. However, the balance between miR396 and its targets was disrupted in flowers of miR396-overexpressing plants, and its target genes were dramatically down-regulated in the flowers, compared with those in wild-type flowers. The altered expressions of *GRF* genes were responsible for the deformed pistils in *35S:MIR396a* plants. When *35S:MIR396a* plants were crossed with *35S:GRF7/9* plants, their progenies, *35S:GRF(7/9)/35S:MIR396a*, displayed phenotypes identical to those of *35S:MIR396a* plants. In contrast, *35S:mGRF7/9* restored *35S:MIR396a* plants to wild-type. Therefore, the right amount of *GRF* levels is required for pistil development. A similar case was also observed in tobacco where over-expression of miR396 caused aberrant pistils via down-regulation of *GRF* targets (Yang et al., 2009; Baucher et al., 2013). We also observed that the narrow leaf phenotypes were always linked with aberrant pistils and elevated *GRF* expression could rescue both defects, implying that the miR396/*GRF*s cascade regulates the development of both leaf and flower. These results revealed that appropriate regulation of *GRF* genes by miR396 is necessary for plant development.

Although we reveal that miR396 affects the development of pistils by regulation of *GRF*s, it is still unclear which developmental processes were linked to the pistil abnormalities. As shown in Fig. 5A, both *GRF*s and *GIF*s were expressed in the early pistil developmental stages. It is likely that the GRF/GIF complexes control the expression of genes involved in early pistil development. Further investigation into the detailed expression patterns of *GRF*s and *GIF*s and to establish the direct targets regulated by the GRF/GIF complexes are required to well understand the mechanism of pistil formation.

MATERIALS AND METHODS

Plant Materials

Arabidopsis ecotype Col-0 was used for all experiments. The generation of *35S:MIR396a* plants were described previously (Liu et al., 2009). Plants were grown in long photoperiods (16 hour light/8 hour dark) or in short photoperiods (8 hour light/16 hour dark) at 23°C

Real-Time qRT-PCR Experiments.

One micrograms total RNA extracted using the Trizol reagent (Invitrogen) was used for oligo(dT)18 primed cDNA synthesis according to the reverse transcription protocol (Fermentas). The resulting cDNA was subjected to relative quantitative PCR using a SYBR Premix Ex Taq^{TM} kit (TaKaRa) on a Roche LightCycler 480 real-time PCR machine, according to the manufacturer's instructions. For each reported result at least three independent biological samples were subjected to minimum of three technical replicates. The results were normalized to *ACT2*. The qRT-PCR primers for 9 GRFs were described previously (Rodriguez et al., 2010).The other qRT-PCR primers used are listed in Table S1.

Plasmid Construction

The pOCA30 binary plasmid was used for an expression vector. For

overexpression, the genome sequence for each gene was cloned into the pOCA30 vector. The miRNA target motif in *GRF7* or *GRF9* was altered, introducing synonymous mutations in a cloned *GRF7* or *GRF9* wild-type genomic fragment.

Yeast Assays

For Y2H assay, all the N-terminal truncated GRFs containing the QLQ and WRC domains were cloned into pGBKT7, and the full-length *GIF*s were cloned into pGADT7. The N terminal sequences of the GRFs for yeast two-hybrid assay can been found according to the primers provided in Table S1. For transactivation assays, the full-length *GRF* and *GIF* cDNAs were cloned into pGBKT7 and introduced into yeast cells. Growth was determined as described in the Yeast Two-Hybrid System User Manual (Clontech). Primers used for the vector construction were listed in Table S1. Experiments were repeated three times.

Agrobacterium tumefaciens* Infiltration in *Nicotiana benthamiana

Plasmids were transformed into *A. tumefaciens* strain EHA105. Agrobacterial cells were infiltrated into leaves of N.benthamiana. For miRNA/GRF coinfiltration experiments, equal volumes of an *Agrobacterium* culture containing *35S:MIR396a* (OD600 = 1.75) and *35S:(m)GRF7/9* (OD600 = 0.25) were mixed before infiltration into *N. benthamiana* leaves. After infiltration, plants were placed at 24°C for 72 h before RNA extraction.

For BiFC assays, full-length coding sequences of *Arabidopsis GRF4*, *GRF7*, *GRF9*, *GIF1*, *GIF2*, and *GIF3* were cloned into the binary nYFP or cYFP vector. Agrobacterium strains transformed with indicated nYFP or cYFP vector were incubated, harvested, and resuspended in infiltration buffer (0.2 mM acetosyringone, 10 mM $MgCl_2$, and 10 mM MES, PH5.6) to identical concentrations (OD600 = 0.5). For miRNA/GRF/GIF interaction test, equal volumes of an agrobacterium culture containing *35S:MIR395a* or

*35S:MIR396*a (OD600 = 2.5), *35S:*(*m*)*GRF7-nYFP* (OD600 = 0.5), and *35S:GIF2-cYFP* (OD600 = 0.5) were mixed before infiltration into *N. benthamiana* leaves. After infiltration, plants were placed at 24°C for 48 h before observation.

CoIP Assay

Flag-GRF-nYFP and Myc-GIF-cYFP (or Myc-cYFP) were transiently co-expressed in *N. benthamiana* leaves. Infected leaves were harvested 48 h after infiltration and used for protein extraction. Flag-fused GRF was immunoprecipitated using Flag antibody and the coimmunoprecipitated proteins were then detected using Myc antibody.

Scanning Electron Microscopy and GUS Assays

For scanning electron microscopy analysis, siliques from flowers at stage 15 were separated, fixed, dehydrated, dried, coated with gold-palladium, and then photographed.

For promoter-GUS constructs of *GRF*s and *GIF*s, about 2kb upstream promoter regions were amplified and fused with the GUS gene. The primers were listed in Table S1. Transgenic plants were subjected to GUS staining as described previously (Liang et al., 2010).

Accession Numbers

MIR396a (AT2G10606), MIR396b (AT5G35407), *GRF1* (AT2G22840), *GRF2* (AT4G37740), *GRF3* (AT2G36400), *GRF4* (AT3G52910), *GRF5* (AT3G13960), *GRF6* (AT2G06200), *GRF7* (AT5G53660), *GRF8* (AT4G24150), GRF9 (AT2G45480), *GIF1* (AT5G28640), *GIF2* (AT1G01160), *GIF3* (AT4G00850), and *ACT2* (AT3G18780). The T-DNA insertion mutants used in this article: *grf1* (SALK_069339C), *grf3* (SALK_026786), *grf4* (SALK_077829C), *grf5* (SALK_086597C), *grf7* (CS878963), *grf8* (CS804312), *grf9* (SALK_140746C), *gif1* (SALK_150407), *gif2* (CS851972), and *gif3* (SALK_052744)

ACKNOWLEDGEMENTS

We thank the editor and two anonymous reviewers for their constructive comments, which helped us to improve the manuscript. We thank the *Arabidopsis* Resource Center at the Ohio State University for the T-DNA insertion mutants. We thank Yanhui Zhao (Kunming Institute of Botany, CAS) for SEM assistance.

LITERATURE CITED

Achard P, Herr A, Baulcombe DC, Harberd NP (2004) Modulation of floral development by a gibberellin-regulated microRNA. Development **131**: 3357-3365

Aizawa H, Hu SC, Bobb K, Balakrishnan K, Ince G, Gurevich I, Cowan M, Ghosh A (2004) Dendrite Development Regulated by CREST, a Calcium-Regulated Transcriptional Activator. Science **303**: 197-202

Aukerman MJ, Sakai H (2003) Regulation of Flowering Time and Floral Organ Identity by a MicroRNA and Its APETALA2-Like Target Genes. Plant Cell **15**: 2730-2741

Baker CC, Sieber P, Wellmer F, Meyerowitz EM (2005) The early extra petals1 mutant uncovers a role for microRNA miR164c in regulating petal number in *Arabidopsis*. Curr Biol **15**:303-315

Bartel DP (2004) MicroRNAs: Genomics, biogenesis, mechanism, and function. Cell 116: 218–297

Baucher M, Moussawi J, Vandeputte OM, Monteyne D, Mol A, Pérez-Morga D, El Jaziri M (2013) A role for the miR396/GRF network in specification of organ type during flower development, as supported by ectopic expression of Populus trichocarpa miR396c in transgenic tobacco. Plant Biol **15**: 892-898.

Brett D, Whitehouse S, Antonson P, Shipley J, Cooper C, Goodwin G (1997) The SYT protein involved in the t(X;18) synovial sarcoma translocation is a transcriptional activator localised in nuclear bodies. Hum Mol Genet **6**: 1559–1564

Brodersen P, Sakvarelidze-Achard L, Brunun-Rasmussen M, Dunoyer P, Yamamoto YY, Sieburth L, Voinnet O (2008) Widespread translational inhibition by plant miRNAs and siRNAs. Science **320**: 1185-1190

Carrington JC, Ambros V (2003) Role of microRNAs in plant and animal development. Science **301**: 336–338

Chen X (2004) A microRNA as a translational repressor of APETALA2 in *Arabidopsis* flower development. Science **303**: 2022–2025

Debernardi JM, Rodriguez RE, Mecchia MA, Palatnik JF (2012) Functional specialization of the plant miR396 regulatory network through distinct microRNA–target interactions. PLoS Genet **8**: e1002419

Horiguchi G, Kim GT, Tsukaya H (2005) The transcription factor AtGRF5 and the transcription coactivator AN3 regulate cell proliferation in leaf primordia of *Arabidopsis thaliana*. Plant J **43**: 68-78

Hewezi, T, Maier TR, Nettleton D, Baum TJ (2012) The *Arabidopsis* microRNA396-GRF1/GRF3 regulatory module acts as a developmental regulator in the reprogramming of root cells during cyst nematode infection. Plant Physiol **159**: 321-335

Jones-Rhoades MW, Bartel DP (2004) Computational identification of plant microRNAs and their targets, including a stress-induced miRNA. Mol Cell **14**: 787-799

Kato H, Tjernberg A, Zhang W, Krutchinsky AN, An W, Takeuchi T, Ohtsuki Y, Sugano S, de Bruijn DR, Chait BT, et al (2002) SYT associates with human SNF/SWI complexes and the C-terminal region of its fusion partner SSX1 targets histones. J Biol Chem **277**: 5498-5505

Kim JH, Choi D, Kende H (2003) The AtGRF family of putative transcription factors is involved in leaf and cotyledon growth in *Arabidopsis*. Plant J **36**:

94-104

Kim JH, Kende H (2004) A transcriptional coactivator, AtGIF1, is involved in regulating leaf growth and morphology in *Arabidopsis*. Pro Natl Acad Sci USA **101**: 13374-13379

Kim J, Jung J, Reyes JL, Kim Y, Kim S, Chung KS, Kim JA, Lee M, Lee Y, Narry Kim V, et al (2005) microRNA-directed cleavage of ATHB15 mRNA regulates vascular development in *Arabidopsis* inflorescence stems. Plant J **42**: 84-94

Kim JS, Mizoi J, Kidokoro S, Maruyama K, Nakajima J, Nakashima K, Mitsuda N, Takiguchi Y, Ohme-Takagi M, Kondou Y, et al (2012) *Arabidopsis* growth-regulating factor 7 functions as a transcriptional repressor of abscisic acid- and osmotic stress-responsive genes, including DREB2A. Plant Cell **24**: 3393-3405

Lanet E, Delannoy E, Sormani R, Floris M, Brodersen P, Crété P, Voinnet O, Robaglia C (2009) Biochemical evidence for translational repression by *Arabidopsis* MicroRNAs. Plant Cell **21**: 1762-1768

Lee BH, Ko J, Lee S, Lee Y, Pak J, Kim JH (2009) The *Arabidopsis* GRF-INTERACTING FACTOR gene family performs an overlapping function in determining organ size as well as multiple developmental properties. Plant Physiol **151**: 655-668

Liang G, Yang F, Yu D (2010) MicroRNA395 mediates regulation of sulfate accumulation and allocation in *Arabidopsis thaliana*. Plant J 62: 1046-1057

Liu D, Song Y, Chen Z, Yu D (2009) Ectopic expression of miR396 suppresses GRF target gene expression and alters leaf growth in *Arabidopsis*. Physiol Plant **136**: 223-236

Liu X, Huang J, Wang Y, Khanna K, Xie Z, Owen HA, Zhao D (2010) The role of floral organs in carpels, an Arabidopsis loss-of-function mutation in MicroRNA160a, in organogenesis and the mechanism regulating its expression. Plant J **62**: 416-428

Mallory AC, Dugas DV, Bartel DP, Bartel B (2004) MicroRNA regulation of

NAC-domain targets is required for proper formation and separation of adjacent embryonic, vegetative, and floral organs. Curr Biol **14**: 1035-1046

Millar AA, Gubler F (2005) The *Arabidopsis* GAMYB-Like genes, MYB33 and MYB65, are microRNA-regulated genes that redundantly facilitate anther development. Plant Cell **17**: 705-721

Reinhart BJ, Weinstein EG, Rhoades MW, Bartel B, Bartel DP (2002) MicroRNAs in plants. Genes Dev **16**: 1616–1626

Rodriguez RE, Mecchia MA, Debernardi JM, Schommer C, Weigel D, Palatnik JF (2010) Control of cell proliferation in *Arabidopsis thaliana* by microRNA miR396. Development **137**: 103-112

Ru P, Xu L, Ma H, Huang H (2006) Plant fertility defects induced by the enhanced expression of microRNA167. Cell Res **16**: 457-465

Schauer SE, Jacobsen SE, Meinke DW, Ray A (2002) DICER-LIKE1: Blind men and elephants in *Arabidopsis* development. Trends Plant Sci **11**: 487-491.

Treich I, Cairns BR, de los Santos T, Brewster E, Carlson M (1995) SNF11, a new component of the yeast SNF-SWI complex that interacts with a conserved region of SNF2. Mol Cell Biol **15**: 4240-4248

Thaete C, Brett D, Monaghan P, Whitehouse S, Rennie G, Rayner E, Cooper CS, Goodwin G (1999) Functional domains of the SYT and SYT–SSX synovial sarcoma translocation proteins and co-localization with the SNF protein BRM in the nucleus. Hum Mol Genet **8**: 585–591

Vaucheret H, Vazquez F, Crete P, Bartel DP (2004) The action of ARGONAUTE1 in the miRNA pathway and its regulation by the miRNA pathway are crucial for plant development. Genes Dev **18**: 1187-1197

Wang L, Gu X, Xu D, Wang W, Wang H, Zeng M, Chang Z, Huang H, Cui X (2011) miR396-targeted AtGRF transcription factors are required for coordination of cell division and differentiation during leaf development in *Arabidopsis*. J Exp Bot **62**: 761-773

Williams L, Grigg SP, Xie M, Christensen S, Fletcher JC (2005) Regulation

of *Arabidopsis* shoot apical meristem and lateral organ formation by microRNA miR166g and its AtHD-ZIP target genes. Development **132**: 3657-3668

Wu M, Tian Q, Reed JW (2006) *Arabidopsis* microRNA167 controls patterns of ARF6 and ARF8 expression, and regulates both female and male reproduction. Development **133**: 4211-4218

Yan J, Gu Y, Jia X, Kang W, Pan S, Tang X, Chen X, Tang G (2012) Effective small RNA destruction by the expression of a short tandem target mimic in *Arabidopsis*. Plant Cell **24**: 415-427

Yang F, Liang G, Liu D, Yu D (2009) *Arabidopsis* miR396 mediates the development of leaves and flowers in transgenic tobacco. J Plant Biol **52**: 475-481

Figure legends

Figure 1. Phenotypes of *35S:MIR396a* plants.

(A) Wild type flower. (B-D) Bent pistil (B), unfused carpels (C), and single-carpel pistil (D) in the flowers of *35S:MIR396a* plants. (E) First 20 siliques in wild type and *35S:MIR396a* plants. The white asterisk indicates the single-carpel siliuqes. (F) Siliques at stage 15 (left) and mature siliques (right). (G) Percentage of siliques containing single-carpel or two-carpel. (H) Percentage of siliques with the indicated number of seeds. Three individuals for each genotype were used for silique analysis. 30 siliques for each individual were analyzed.

Figure 2. Regulation of *GRF*s by miR396

(A) Transcript levels of *GRF*s in flowers. (B) Transcript levels of *MIR396*s and *GRF*s in sepal, petal, stamen, and pistil at floral stage 13. (C) Transcript levels of *MIR396*s and *GRF*s in pistil at the indicated floral stages. (D) Coexpression of various combinations of *MIRNA* and *GRF* expression constructs in *N. benthamiana*. (A-D) Error bars represent SE for three independent

experiments. The values marked by an asterisk are significantly different from the control values ($P < 0.01$; $n = 3$).

Figure 3. Rescue of *35S:MIR396a* by *mGRF*

(A) Six representative siliques were presented for each plant. The white asterisk indicates the single-carpel siliques. (B) Expression of GRF7 and GRF9. Flowers of F1 progenies for indicated two parental plants were used for expression analysis. Error bars represent SE for three independent experiments. The values marked by an asterisk are significantly different from the control values ($P < 0.01$; $n = 3$).

Figure 4. Interaction of GRFs and GIFs.

(A) Yeast two-hybrid assays. Interaction was indicated by the ability of cells to grow on synthetic dropout medium lacking Leu/Trp/His/Ade. N-terminal truncated GRFs and full-length GIFs were cloned into pGBKT7 and pGADT7, respectively. (B) BiFC assays. Fluorescence was observed in nuclear compartments of *N.benthamiana* leaf epidermal cells; the fluorescence resulted from complementation of the N-terminal portion of YFP fused to GRF (GRF-nYFP) with the C-terminal portion of YFP fused to GIF (GIF-cYFP). (C) CoIP assays. Flag fused GRF-nYFP was immunoprecipitated using Flag antibody, and co-immunoprecipitated Myc-GIF-cYFP was then detected using Myc antibody.

Figure 5. Tissue-specific expression of *GRF*s and *GIF*s.

(A) Inflorescence staining of indicated genes. (B) Expression of *GIF*s in sepal, petal, stamen, and pistil at floral stage 13. (C) Expression of *GIF*s in pistils at the indicated floral stage.

Figure 6. miR396 suppresses formation of the GRF/GIF complex.

MIRNA, *(m)GRF7-nYFP*, and *GIF2-cYFP* constructs were co-infiltrated into

774 tobacco epidermal cells as described in method. *MIR395a* was used as a
775 negative control.
776
777 **Figure 7**. *gif1/2/3* triple mutants mimic *35S:MIR396a/grf5*.
778 (A) Pistil with unfused carpels in *gif1/2/3* mutants. (B) Single-carpel pistil in the
779 *gif1/2/3* flower. (C) Normal siliques (left, WT) and single-carpel silique (right,
780 *gif1/2/3*). (D) Representative siliques for the indicated plants. The white
781 asterisk indicates the single-carpel siliuqes. (E) Percentage of siliques
782 containing single-carpel or two-carpel. Three individuals for each genotype
783 were used for silique analysis. 30 siliques for each individual were analyzed.

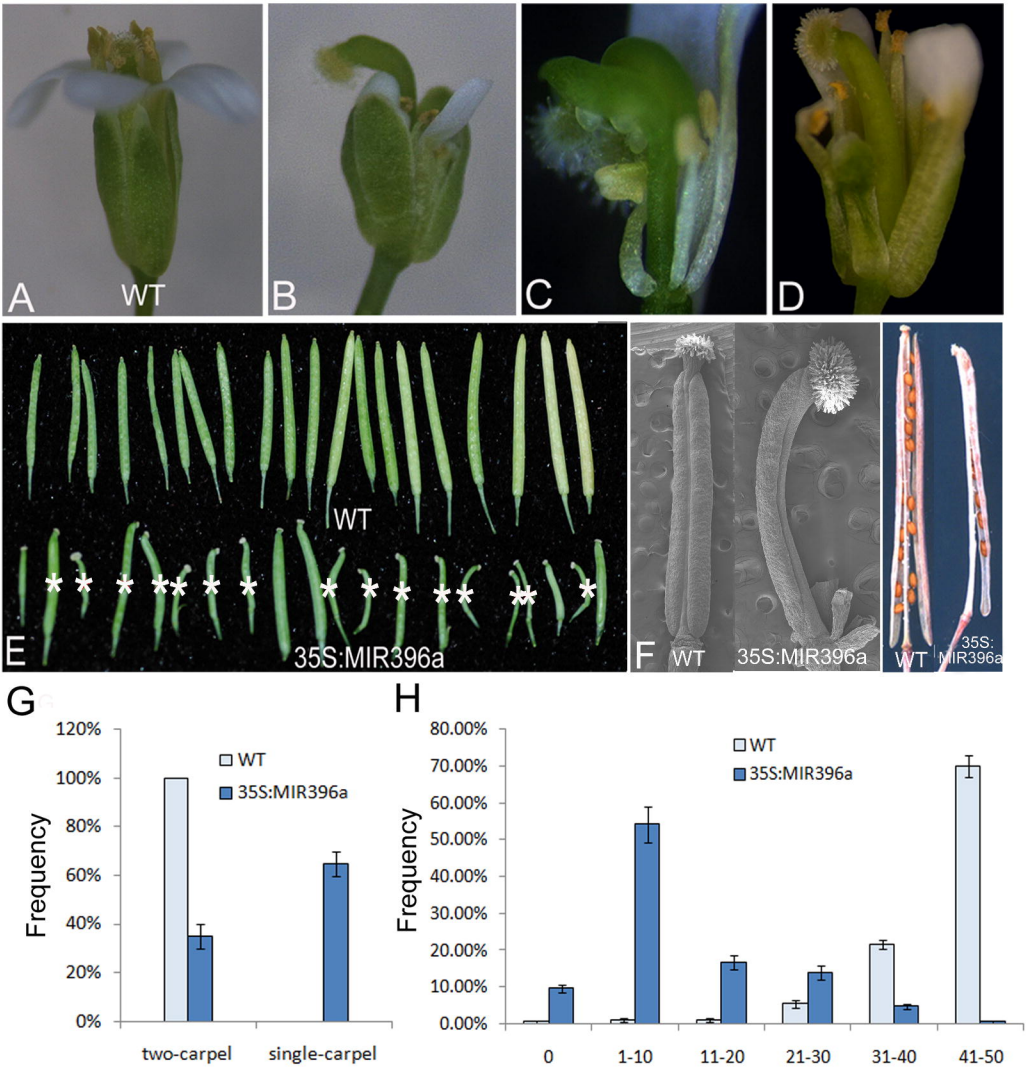

Figure 1. Phenotypes of 35S:MIR396a plants.

(A) Wild type flower. (B-D) Bent pistil (B), unfused carpels (C), and single-carpel pistil (D) in the flowers of 35S:MIR396a plants. (E) First 20 siliques in wild type and 35S:MIR396a plants. The white asterisk indicates the single-carpel siliuqes. (F) Siliques at stage 15 (left) and mature siliques (right). (G) Percentage of siliques containing single-carpel or two-carpel. (H) Percentage of siliques with the indicated number of seeds. Three individuals for each genotype were used for silique analysis. 30 siliques for each individual were analyzed.

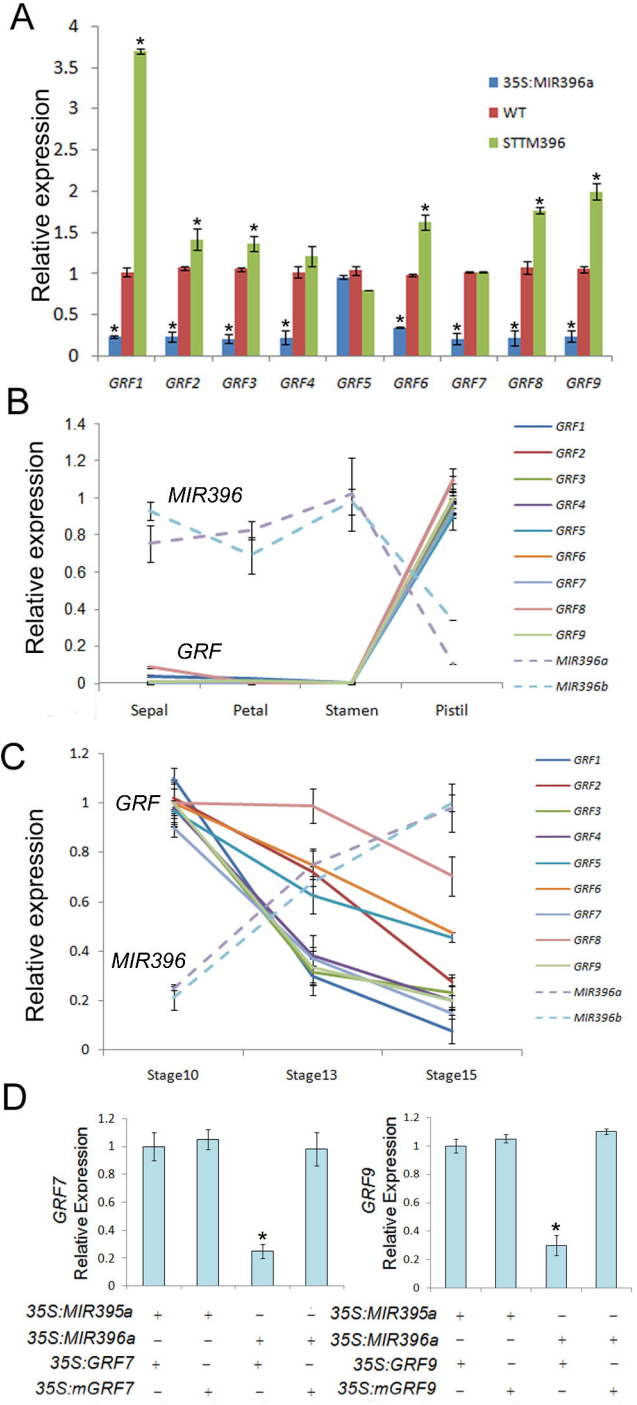

Figure 2. Regulation of GRFs by miR396

(A) Transcript levels of GRFs in flowers. (B) Transcript levels of MIR396s and GRFs in sepal, petal, stamen, and pistil at floral stage 13. (C) Transcript levels of MIR396s and GRFs in pistil at the indicated floral stages. (D) Coexpression of various combinations of MIRNA and GRF expression constructs in N. benthamiana. (A-D) Error bars represent SE for three independent experiments. The values marked by an asterisk are significantly different from the control values ($P < 0.01$; $n = 3$).

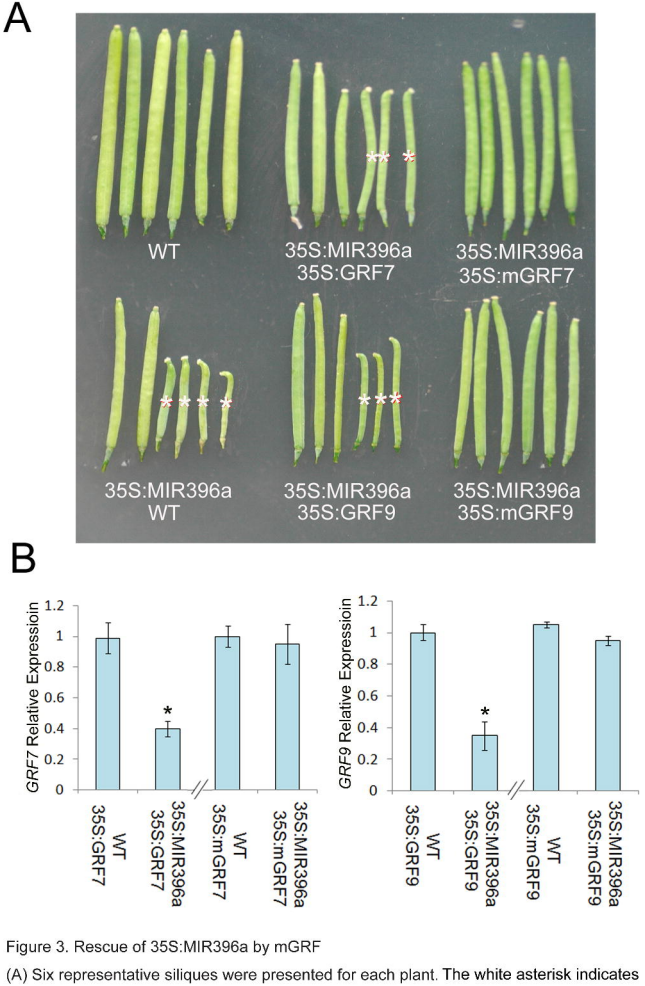

Figure 3. Rescue of 35S:MIR396a by mGRF

(A) Six representative siliques were presented for each plant. The white asterisk indicates the single-carpel siliques. (B) Expression of GRF7 and GRF9. Flowers of F1 progenies for indicated two parental plants were used for expression analysis. Error bars represent SE for three independent experiments. The values marked by an asterisk are significantly different from the control values ($P < 0.01$; $n = 3$).

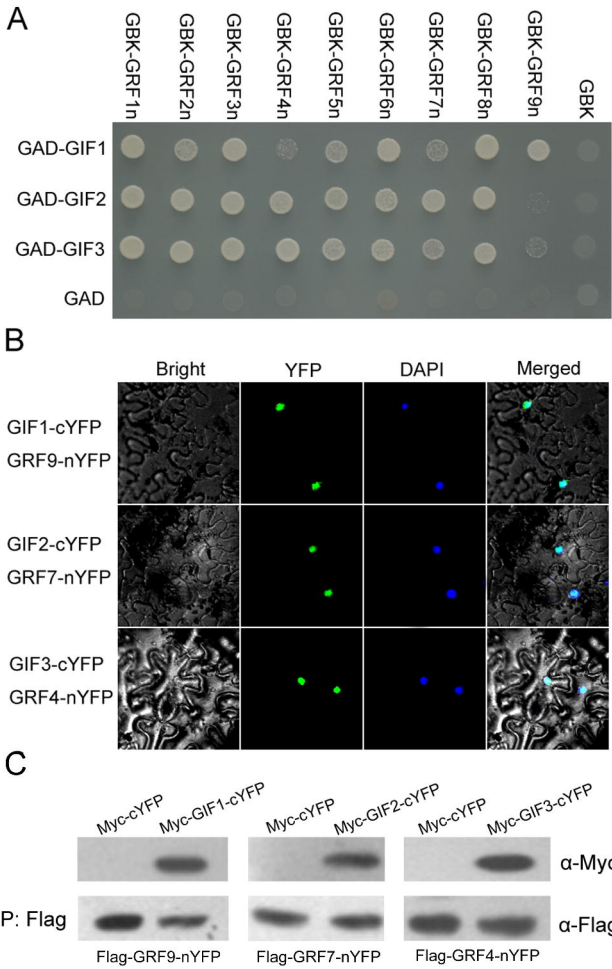

Figure 4. Interaction of GRFs and GIFs.

(A) Yeast two-hybrid assays. Interaction was indicated by the ability of cells to grow on synthetic dropout medium lacking Leu/Trp/His/Ade. N-terminal truncated GRFs and full-length GIFs were cloned into pGBKT7 and pGADT7, respectively.

(B) BiFC assays. Fluorescence was observed in nuclear compartments of N.benthamiana leaf epidermal cells; the fluorescence resulted from complementation of the N-terminal portion of YFP fused to GRF (GRF-nYFP) with the C-terminal portion of YFP fused to GIF (GIF-cYFP).

(C) CoIP assays. Flag fused GRF-nYFP was immunoprecipitated using Flag antibody, and co-immunoprecipitated Myc-GIF-cYFP was then detected using Myc antibody.

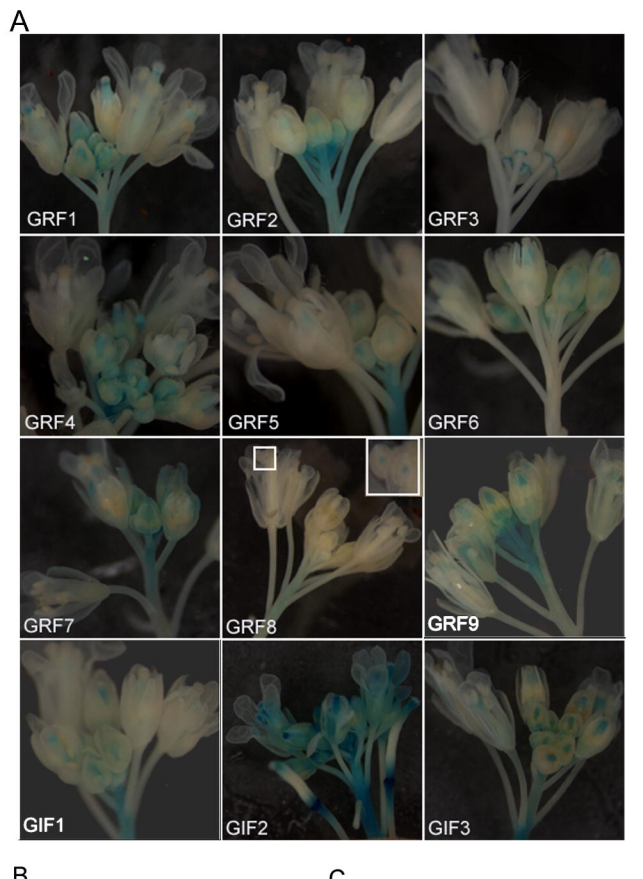

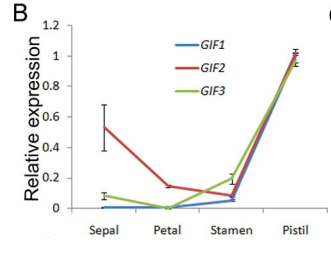

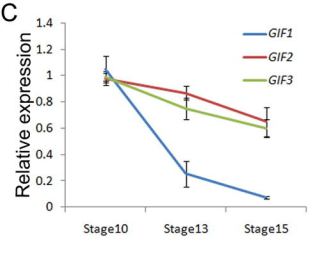

Figure 5. Tissue-specific expression of GRFs and GIFs.

(A) Inflorescence staining of indicated genes. (B) Expression of GIFs in sepal, petal, stamen, and pistil at floral stage 13. (C) Expression of GIFs in pistils at the indicated floral stage.

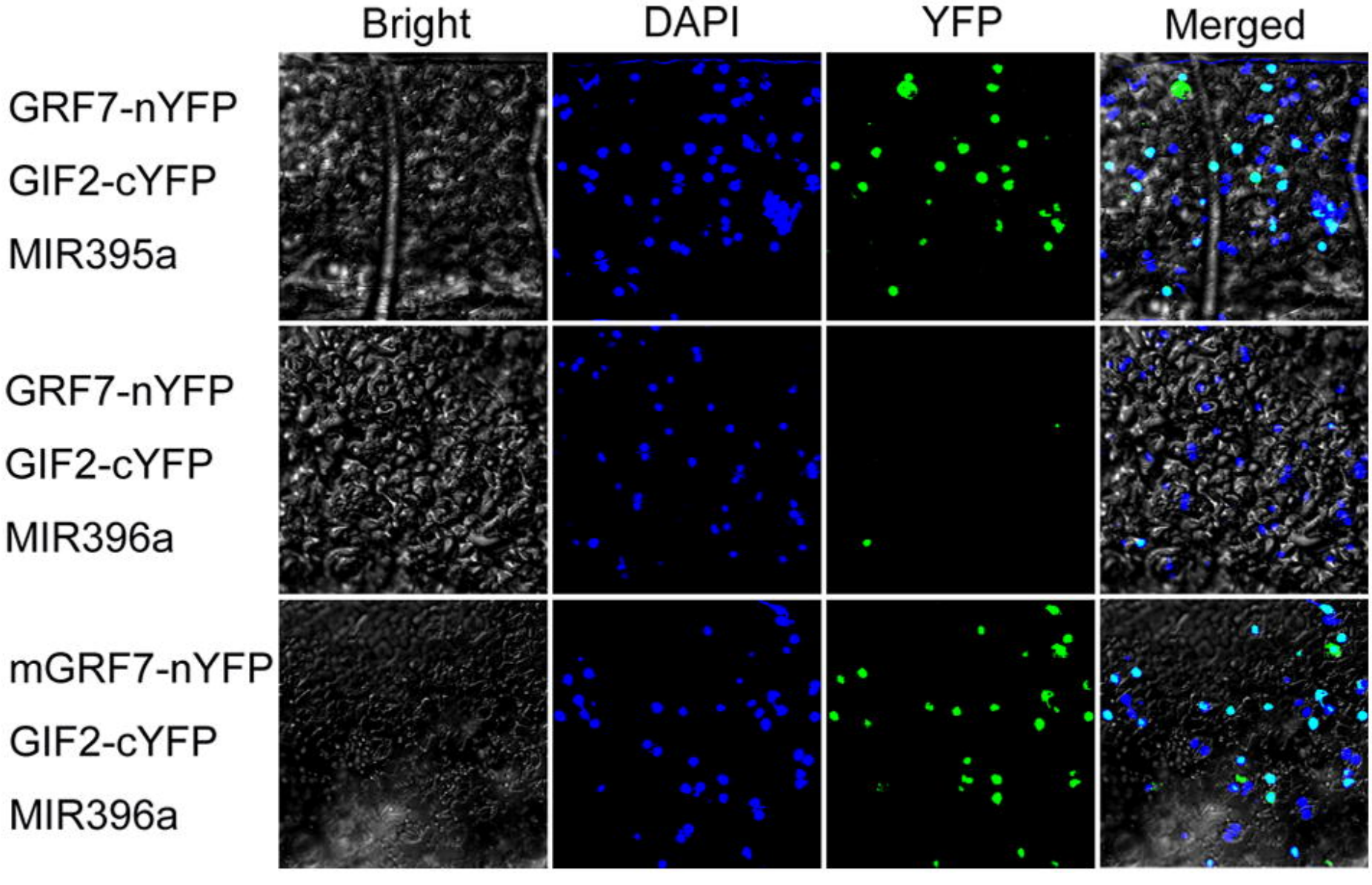

Figure 6. miR396 suppresses formation of the GRF/GIF complex.

MIRNA, (m)GRF7-nYFP, and GIF2-cYFP constructs were co-infiltrated into tobacco epidermal cells as described in method. MIR395a was used as a negative control.

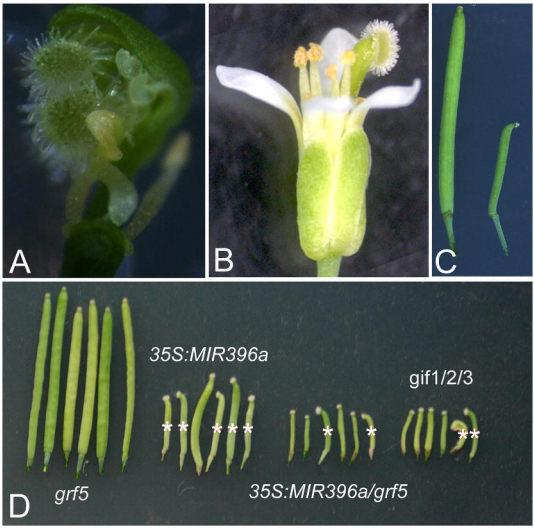

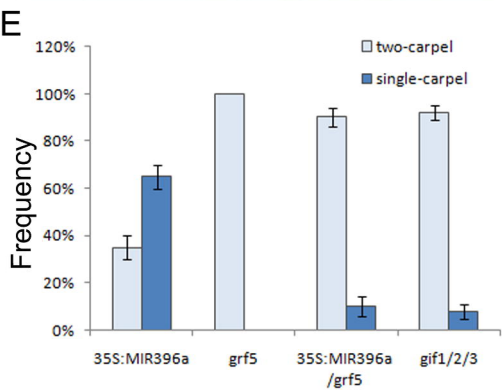

Figure 7. gif1/2/3 triple mutants mimic 35S:MIR396a/grf5.
(A) Pistil with unfused carpels in gif1/2/3 mutants. (B) Single-carpel pistil in the gif1/2/3 flower. (C) Normal siliques (left, WT) and single-carpel silique (right, gif1/2/3). (D) Representative siliques for the indicated plants. The white asterisk indicates the single-carpel siliuqes. (E) Percentage of siliques containing single-carpel or two-carpel. Three individuals for each genotype were used for silique analysis. 30 siliques for each individual were analyzed.